Performance of a Multiband Passive Bistatic Radar Processing Scheme - Part II

Karl Erik Olsen and Karl Woodbridge

(Invited Paper)

Abstract

This work is based on the premise that it is possible to improve on the Passive Bistatic Radar (PBR) range resolution by exploiting the full broadcast bandwidth from transmitters of opportunity. The work shows how the exploitation of the available frequency scattered bandwidth from single broadcast towers can be achieved by coherently by combining each of the individual channels/bands, and that the range resolution is improved accordingly. Part I of this work presented an analysis of the algorithm on how to combine non-adjacent single channels/bands in the range correlation, and here performance simulations based on real life signals from both Frequency Modulated (FM) radio and Digital Video Broadcast - Terrestrial (DVB-T) signals are presented.

I. INTRODUCTION

This paper is presenting simulated performances based on real life signals of the multiband algorithm presented in part I of this work, [1]. Full details and further reading may be found in [2]–[5].

The proposed processing scheme is inspired by the high range resolution approaches used in High Range Resolution (HRR) radar systems, on how to exploit multiple non-adjacent broadcast channels/bands in the Passive Bistatic Radar (PBR) range correlation in order to achieve higher range resolution, while maintaining the Doppler resolution from the relatively long integration

K. E. Olsen, Norwegian Defence Research Establishment, P O Box 25, NO-2027 Kjeller, Norway e-mail: karl-erik.olsen@ffi.no.

K. Woodbridge, University College London, Department of Electronic & Electrical Engineering, University College London, Torrington Place, London, WC1E 7JE, United Kingdom, e-mail: k.woodbridge@ee.ucl.ac.uk.

times. The broadcast channels/bands are assumed to be from a single transmitter. The following problems were addressed and solved, [1]–[5]:

- By using broadcast signals at different carrier frequencies, the target Doppler shift will be different, and the proposed method takes this into account.

- By using time varying waveforms (signals of opportunity, i.e. Frequency Modulated (FM), Digital Audio Broadcast (DAB), Digital Video Broadcast - Terrestrial (DVB-T), or pseudo noise) in the range correlation, a time varying result is achieved. If this becomes an issue, it should be countered by increasing the range correlation time. This might be achieved either by increasing the total Coherent Processing Interval (CPI), or by keeping the total CPI constant and reducing the Doppler resolution while increasing the range correlation time.

- Combining multiple bands results in co-channel correlation as well as cross-channel correlation. While only the former is sought, it was showed that the cross terms may be neglected due to their correlation properties with respect to each other. This is also helped by the fact that they contain a destructive frequency component from the de-modulation.

- Even though good individual correlation performances are achieved for single channels/bands, summing the correlation contributions for the different channels/bands might cause an out of phase summation which will modulate the range correlation peak in a way that may cause erroneous range estimates. The algorithm estimates a phase correction term that once applied, makes all contributions in phase, and thus erroneous range estimates, as well as destructive summing of target responses, are avoided.

The method was tested on pseudo random generated noise signals with FM radio and DVB-T like parameters [1]. The pseudo random noise signals were chosen in order to some extent use a predictable code in the presentation of the algorithm. The FM radio signals are highly time varying signals, and the DVB-T signal contains deterministic components that results in predictable ambiguities [6, pp. 315-338]. In order to mitigate these signal specific effects in the performance presentation of the algorithm, a pseudo random noise signal which behaved predictable was generated.

In summary, [1] showed the development of a processing scheme enabling the simultaneous processing of multiple broadcast channels in order to improve the range correlation's bandwidth.

The algorithm has been derived mathematically and tested using simulated signals, and this work forms the basis for developing high range resolution imaging and Inverse Synthetic Aperture Radar (ISAR) capabilities in the PBR systems under consideration.

II. FM RADIO WAVEFORM ANALYSIS

The focus of this work is to exploit multiple channels from the same FM radio tower, and the algorithm was explained briefly in [1], [7] for a pseudo random noise signal. This section applies real recorded FM radio signals to gain insight into the algorithm's performance using FM radio signals. The reference antenna is pointed at a strong nearby transmitter, and thus a strong and clear signal is recorded. The signal potentially contains multipath, even though it is diffracted from transmitter to receiver. The sampled reference signal is digitally substituted in the surveillance signal, and thus the following situation is achieved: Data analysis with real life propagation, full match with the reference and surveillance channel's signals, and thus the FM radio waveform's performance is analyzed. Schematics of the FM radio receiving system is illustrated in figure 1. The full FM radio band is sampled, and individual channels of interest are extracted and processed according to the proposed processing scheme. The parameters B and Δf are the selected bandwidth and the selected center-to-center frequencies of the synthetic range correlated signal, [1].

Figure 2 shows the schematic diagram of the decoded FM radio signal or unmodulated information signal. The information signal is occupying $100kHz$, and it consists of multiple parts. Ranging from $30Hz$ to $15kHz$ is the mono audio section, which consists of the sum of the stereo left and right channels. This is the part which all FM radio receivers can decode. Then there is the $19kHz$ stereo pilot, which has two functions: First the mere presence decides whether the transmission is stereo or mono by definition. Second, if the pilot is present, this carrier is used in the receiver to decode the stereo audio as seen as the double sideband centered at $38kHz$, ranging from $23kHz$ to $53kHz$, being the difference of the stereo left and right channels. And also, the double sideband modulated Radio Data System (RDS) information at $57kHz = 3 \times 19kHz$. In the rest of the band national adaptations may apply, and in our recordings, no traces of a regular broadcast signal above the RDS information have been found.

The basics of the FM radio waveform may be found in [10], and in particular the FM modulation. Various bandwidth considerations emerging from the communication research, is
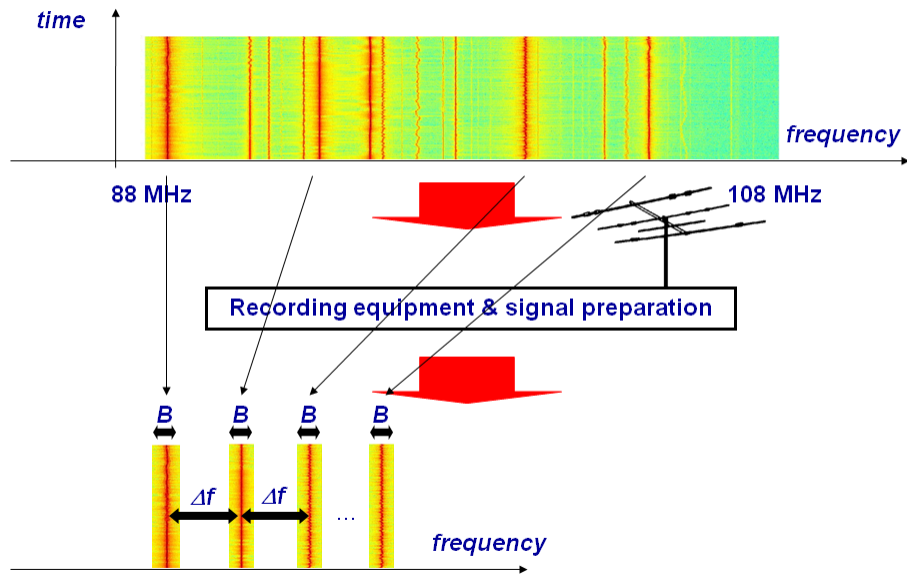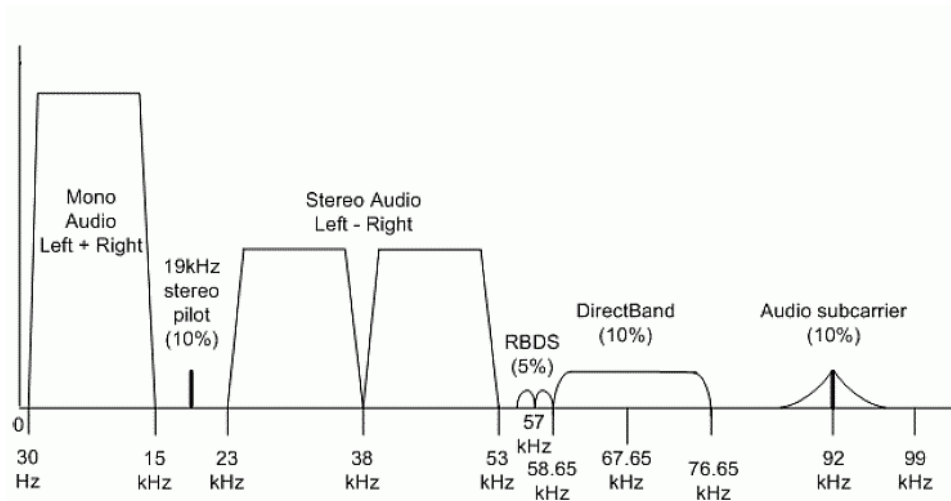
Fig. 1.   Schematics of the FM radio case.

Fig. 2.   Schematic diagram of the frequency content of the decoded FM radio signal or the unmodulated information signal.
National adaptations may apply [8]. The figure is from [9].

(a) $88.7MHz$.

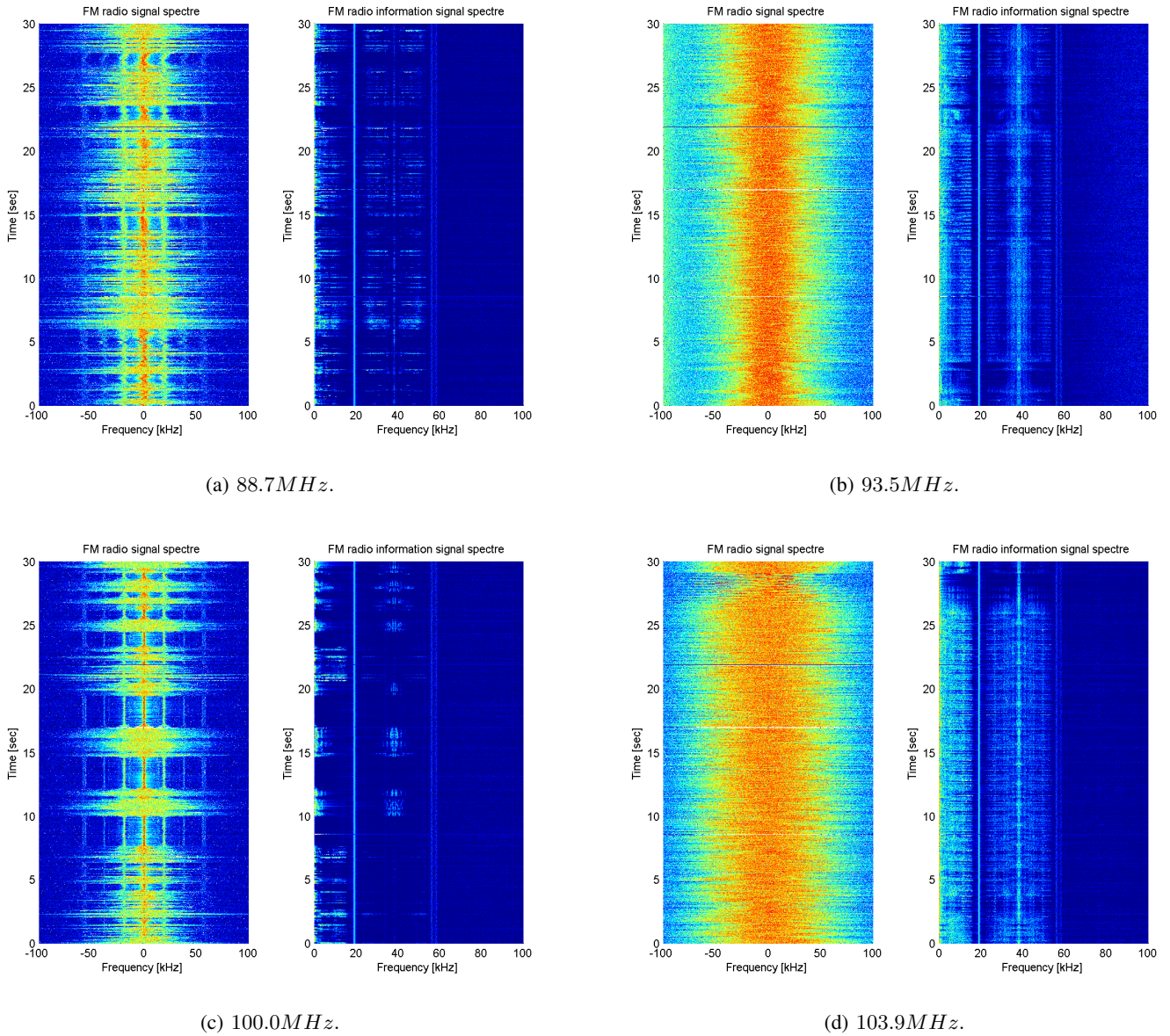(b) $93.5MHz$.

(c) $100.0MHz$.

(d) $103.9MHz$.

Fig. 3. The left sub figures show 30 seconds of the FM radio signal, while the right sub figures show the corresponding decoded FM radio signal, figure 2.

presented, and it may be shown that these considerations are not suitable for radar purposes, as they are focusing on providing sufficient bandwidth for proper channel quality and stability, while efficiently exploiting the limited frequency band available.

The FM radio signal is highly time varying, as seen in figure 3, and further summarized in table I, resulting from a FM software radio demodulation algorithm [11], which was used in

TABLE I

PROGRAM CONTENT AND DESCRIPTION OF THE FM RADIO CHANNELS.

Frequency	Program content and description
$88.7MHz$	Two men talking calmly together in studio.
$93.5MHz$	Music, the group Guns N' Roses playing the former hit "Paradise City"
$100.0MHz$	Man talking very calmly in studio, then playing chanting.
$103.9MHz$	Music, the group No Doubt playing the former hit "Don't speak".

order to produce figure 3, as well as listen to the audio in the recorded signals, table I.

Figure 3's left sub figures show 30 seconds of the FM radio signal, while the right sub figures show the corresponding decoded FM radio signal, as illustrated in figure 2. Table I gives a high level description of the program content of each of the channels. The bandwidth of the FM radio signal with respect to program content has been extensively covered in the literature [12]–[19]. However, figure 2 may lead to the conclusion that a stereo signal has a wider bandwidth than the mono signal, and thus are better suited for radar applications. Looking at figure 3 it is clearly seen that this is not necessarily the case. All shown broadcast signals are stereo signals by definition since the $19kHz$ stereo pilot clearly is present. But only the two music playing channels, figure 3b and d contain substantial stereo information in the stereo audio band $23kHz - 53kHz$. Figure 3a shows scattered stereo information, while (c) shows nearly no stereo information, even though both signals by definition are containing stereo information. The presence of the $19kHz$ stereo pilot is a necessary but not sufficient condition for the presence of signal in the stereo audio channel. In summary, the stereo signal may be broadcasting a close to mono signal as the stereo information is broadcasted as the sum $30Hz - 15kHz$ and difference $23kHz - 53kHz$ of the stereo audio channels, at different parts of the band.

It is also noted that especially in figure 3c, that when there is no or low bandwidth in the information signal, distinct lines appear at the integer value of the $19kHz$ stereo pilot. This is not a hardware failure, and it is explained mathematically in [10, pp. 316-319].

TABLE II

AMBIGUITY DISTANCE $c/\Delta f$, COMBINED WAVEFORM RESOLUTION $c/(N\Delta f)$ AND SAMPLING RESOLUTION c/f_s, FOR $N = 4$.

$[kHz]$ Δf	Ambiguity distance $c/\Delta f$	Combined distance $c/(N\Delta f)$	Sampling distance c/f_s	Ratio $f_s/\Delta f$	Ratio $\frac{f_s}{N\Delta f}$
50	$6000m$	$1500m$	$750.0m$	8.0	2.0
150	$2000m$	$500m$	$375.0m$	5.3	1.3
300	$1000m$	$250m$	$187.5m$	5.3	1.3

The theoretical formula from literature for stepped continuous wave signals range resolution ($-4dB$ width) is [20, pp. 148], combined with the radar world's definition of the resolution to be the half $-3dB$-width (divide by two)

$$\Delta R = \frac{c}{2N\Delta f}, \tag{1}$$

where c is the speed of propagation, N is the number of combined channels, and Δf is the difference in the down modulated bands as described in figure 1, analysed in [1] and full details in [2]–[5]. Table II summaries the expected performance for the chosen parameters. The range ambiguities are expected to be occurring at

$$R_{ambiguity} = R \pm K\frac{c}{\Delta f}, \tag{2}$$

for $K = 0, 1, 2, \ldots$ for a single point target. The signal's bandwidth mainly contributes to lower the sidelobes of the ambiguities, while it is the frequency distance between the signals that defines the main target peak.

Finally, before simulations with real life signals, it should be noted that the highly time varying FM radio signal makes simulations/analysis challenging, as one ends up with all kinds of possible combinations of signal bandwidth, number of channels, carrier frequencies, program contents and so on. The FM radio work in this chapter is based on four individual FM radio channels for a 10 seconds time segment containing a representative mix of variations of bandwidths and program types, as seen in figure 3 and described in table I.

TABLE III

SYNTHETIC TARGET PARAMETERS FOR THE FM RADIO CASE.

Δf [kHz]	Target 1 $v = 100m/s$	Target 2 $v = 100m/s$
$50kHz$	$R = 15.0km$, $0dB$	$R \in [15.0, 21.0]km$, $-3dB$
$150kHz$	$R = 15.0km$, $0dB$	$R \in [15.0, 17.0]km$, $-3dB$
$300kHz$	$R = 15.0km$, $0dB$	$R \in [15.0, 16.0]km$, $-3dB$

A. FM radio waveform, single point target

Table III presents the synthetic target parameters. The surveillance channel contains a time delayed replica of the reference channel, and thus for the single scatterers case, this actually is a range offset autocorrelation function for the reference channel. According to (2) there will be range ambiguities around the target for each $\pm c/\Delta f$. In Doppler, the resolution depends only on the coherent processing interval, at least for processing intervals of interest, i.e. CPI$\leq 1sec$. It is found for this FM radio example that between the expected ambiguities around $15dB$ of dynamic range can be achieved. I.e. in order to resolve two targets in range with a range difference below the ambiguity distance, they have to be below $15dB$ in signal level difference, but probably much less. The next section looks at the behavior when two point targets are present.

Table IV shows the results for one CPI=$328ms$, which behaves roughly as for other CPIs. In order to see the performance as a function of time, the width of the target main peak as a function of time and the $-3dB$, $-6dB$, and $-9dB$ points on each side of the main target peak has been extracted. The latter taken to be the closest sampling value exceeding the required threshold. The results can be seen in table IV for the single channels of $88.7MHz$, $93.5MHz$, $100.0MHz$, and $103.9MHz$, as well as the coherently combination of these channels for $\Delta f = 50kHz$, $\Delta f = 150kHz$, and $\Delta f = 300kHz$.

Table IV summarizes the $-3dB$, $-6dB$, and $-9dB$ points on each side of the main target peak at $15km$ for a dataset corresponding to the first $10sec$ of figure 3. It is seen that the target is stable, but the resolution is highly time varying. The two music playing channels, $93.5MHz$ and $103.9MHz$, are performing best, i.e. $-3dB$ bistatic range target peak width below $5km$, while the two channels containing speech both have corresponding peak widths above $10km$. By

TABLE IV

AUTOCORRELATION PEAK WIDTH FOR SINGLE CHANNEL AS WELL AS FOR THE COMBINED CHANNELS WITH $N = 4$.

		$-3dB$ peak width	$-6dB$ peak width	$-9dB$ peak width
Single channel	$88.7MHz$	$> 10.0km$	$> 10.0km$	$> 10.0km$
	$93.5MHz$	$5.0km$	$8.0km$	$10.0km$
	$100.0MHz$	$> 10.0km$	$> 10.0km$	$> 10.0km$
	$103.9MHz$	$3.4km$	$4.6km$	$6.0km$
Multi channel	$\Delta f = 50kHz$	$1.500km$	$1.500km$	$3.000km$
	$\Delta f = 150kHz$	$0.750km$	$0.750km$	$1.500km$
	$\Delta f = 300kHz$	$0.375km$	$0.375km$	$0.750km$
		Sampling resolution		
		f_s	c/f_s	
Single channel	$88.7MHz$	$1600kHz$	$187.5m$	
	$93.5MHz$	$1600kHz$	$187.5m$	
	$100.0MHz$	$1600kHz$	$187.5m$	
	$103.9MHz$	$1600kHz$	$187.5m$	
Multi channel	$\Delta f = 50kHz$	$400kHz$	$750m$	
	$\Delta f = 150kHz$	$800kHz$	$375m$	
	$\Delta f = 300kHz$	$1600kHz$	$187.5m$	

applying the algorithm, it is not only seen that the resolution is stable with time, the resolution is also improved with respect to the single channel case. For the three cases of combination parameters $\Delta f = 50kHz$, $\Delta f = 150kHz$, and $\Delta f = 300kHz$, the corresponding bistatic target peak widths are now $1.500km$, $0.750km$, and $0.375km$ respectively.

Table IV may lead to the conclusion that the resolutions are not in correspondence with the theory, but that is not the case. The closest range sample that fulfills the target range resolution requested width, being either $-3dB$, $-6dB$, or $-9dB$ is taken as the peak width. This is usually the case in real life systems, as the sampling frequency is tuned against the signal bandwidth.

However, by interpolating between samples and extracting the true $-3dB$ range bandwidth, the performance of the real life data is in accordance with (1).

However, it should be noted that the resolution is the ability to separate two echoes. In the case of a single target/scatterer, the important parameters are accuracy and lack of ambiguities. The latter is described in (2), while the former is just like for other radars, i.e. a function of the available signal-to-noise ratio as described in [21, pp. 5, accuracy].

B. FM radio waveform, two point targets

The ability to resolve two targets in range will be investigated in this section. The surveillance channel is synthesized by combining time/Doppler/amplitude adjusted replicas of the reference channel according to table III. And thus the surveillance channel is time-delayed N range bins, amplitude adjusted, and phase adjusted according to the delay and carrier and target Doppler frequency. This means a second point target at another distance, but the same velocity, is mimicked. The time delay has been adjusted in accordance with the reference/surveillance channel's sampling frequency in order to avoid interpolating the delayed signal between sampling points. This was also found convenient in order to avoid rounding the delay to the same nearest range sampling for adjacent second target delays.

The second target is not resolved in any of the individual FM radio channels, $88.7MHz$, $93.5MHz$, $100.0MHz$, or $103.9MHz$, except from some scattered occurrences in channel $103.9MHz$. In the other channels the target is seen to impact on the correlation peak in the range-Doppler plot, but it is definitely not resolved throughout the systematic delaying the second target between $R = 15.0km$ and $R = 21.0km$.

Figure 4 shows the results of systematic delaying the second target between the first target range at $R = 15.0km$, and the Target 2 end range parameters of table III. The two targets relative levels are also tabulated, and in the following plots, a difference of $3dB$ between the two scatterers to be presented has been chosen.

Figure 4 is interpreted as follows: The first target is at $15km$, while the second target is stepped in range, and the actual target range is indicated in the leftmost column of the plots, numbers edgewise, i.e. the numbers $15.000, 15.750, \ldots, 20.250$. Next/below to these numbers is the dataset duration in seconds, i.e. the numbers 0 and 5. The x-axis of the plots, is the processing range in kms, in (a) i.e. ranging from $14km$ to $21km$.

The range resolution should be as in (1) according to theory for a single point target as also verified in previous section. The figure shows multiband processing for three variations of Δf, for $\Delta f = 50kHz$, $\Delta f = 150kHz$, and $\Delta f = 300kHz$, ten seconds of the dataset seen in figure 3. Figure 4 shows target position 1 at $15km$, and then the second target is stepped systematically from target 1 to the first range ambiguity in steps of the sampling resolution's corresponding range. This means that even though all plots in figure 4 are from different Δf, the overall figure is close to normalized with respect to the ambiguity distance, which is the range interval of interest.

Looking at figure 4a it is seen that the second target is fully resolved from $17.25km$ to $18.75km$, which yields a target peak-to-peak full resolution capability of $2.25km$ between targets differing by $3dB$. Passing $18.75km$, the target is approaching the range ambiguity at $21.000km$.

In figures (b) and (c) there is something going on. The second target is clearly there, a comparison with the single target situation, i.e. $15.000km$, verifies that. The range of the second scatterer seems to be wrong, and no good explanation for this has been found. The analyzed dataset is ten seconds so it is not believed that this is a waveform issue, nor is it expected to be a simulation artifact. Table II shows the ratios $f_s/\Delta f$, and $f_s/(N\Delta f)$, which for the $\Delta f = 150kHz$, and $\Delta f = 300kHz$ is the same and lower $(5.3/1.3)$ than for the $\Delta f = 50kHz$ case $(8.0/2.0)$. Most likely, the algorithm is breaking down as a function of signal input in combination with some simulation artifacts, i.e. very black/white situations. For target multiple scatterers resolution, with the FM radio waveforms the ratios $f_s/\Delta f$, and $f_s/(N\Delta f)$ should be noted, and they should not be too low, and the line might have crossed for $\Delta f = 150kHz$ and $\Delta f = 300kHz$. This is also common sense, as just increasing Δf will not result in the corresponding range resolution capabilities, also due to the fact that the range ambiguities will come closer, but at some point there should be some signal bandwidth present in order to resolve targets.

C. FM radio waveform, summary

The straightforward technique of interpolating to the correlation peak is not resolving targets, only improving on the single target's position. By improving the range resolution one of the major shortfalls of current FM radio based PBR systems is countered. Although the good Doppler resolution of such systems is helping resolving targets, the ability to exploit the better range
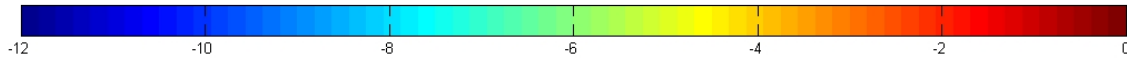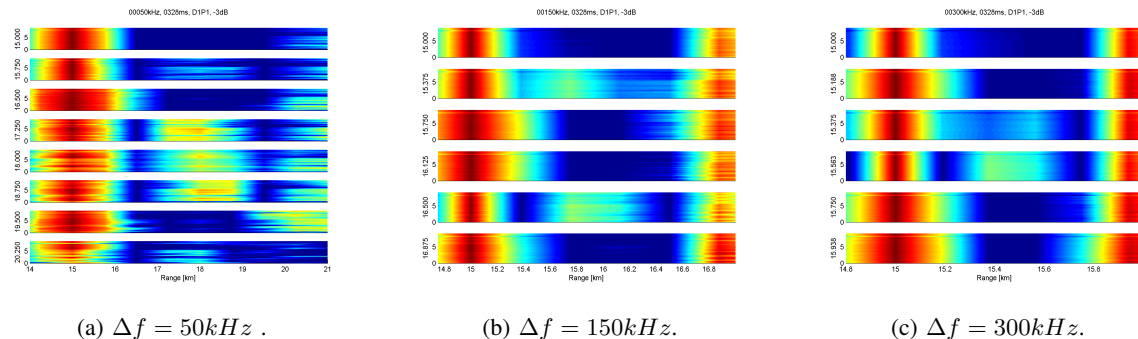
The figure's color coding in dB.

(a) $\Delta f = 50kHz$.   (b) $\Delta f = 150kHz$.   (c) $\Delta f = 300kHz$.

Fig. 4. Systematic testing of the algorithm's resolution capabilities for two scatterers varying according to table III. CPI$= 329ms$, $N = 4$.

resolution for targets at exactly the same velocity and close in range should be able to aid the tracking process.

Simulations based on real life FM radio waveforms show that the algorithm is capable of improving the range resolution according to theory for single scatterers as is summarized in table IV. For multiple scatterers, the algorithm is impacted by the FM radio's time varying behavior. The bandwidth contributes to lowering the range ambiguities sidelobes, and as the bandwidth is fluctuating, the sidelobes are fluctuating as well. Our results indicate that the Δf-parameter should be kept as low as possible when the FM radio waveform is exploited.

The simulations showed no real performance improvement by increasing the coherent integration interval. Some "averaging" effects were observed, as more data is processed together, but no significant performance improvements were observed.

By exploiting multiple broadcast channels the simulations show that the single point scatterer resolution is improved from $3km - 10km+$ for the single channels target peak widths down to $1.5km/0.750km/0.375km$, for the $\Delta f = 50kHz/150kHz/300kHz$ case. All results are tabulated in table IV.

Although care should be taken when applying the algorithm with the FM radio waveform, we shoved that two targets separated down to $2.25km$ were resolved by exploiting four multiple FM radio channels. These two targets were not resolved in any of the individual exploited FM

TABLE V

SYNTHETIC TARGET PARAMETERS FOR THE DVB-T CASE.

Δf	Target 1 $v = 100m/s$	Target 2 $v = 100m/s$
$4MHz$	$R = 15.0km, \, 0dB$	$R \in [15.0, 15.1]km, \, -3dB$
$8MHz$	$R = 15.0km, \, 0dB$	$R \in [15.0, 15.1]km, \, -3dB$

radio channels.

III. DVB-T WAVEFORM ANALYSIS

This chapter presents the performance analysis of the DVB-T radio waveform using the algorithm presented in [2]–[5]. It will be shown that the proposed algorithm offers improved range resolution capability as previously demonstrated for FM transmissions. All analysis are based on real recorded signals from nearby strong transmitters of opportunity.

The generation of the DVB-T signal is well described in [22], and the ambiguity behavior properly treated in [6], [17]. The relatively high bandwidth of DVB-T combined with the relatively long integration times may cause range and Doppler walk, and strategies for meeting those are treated in [23], [24]. These publications are interesting once improved range resolution and/or increased integration times are sought.

In order to show the potential of the DVB-T waveform, a nearby and powerful transmitter was used as signal source for the simulations. The signal was recorded and then synthetic targets according to table V were generated, and the results are presented in the following sections. Schematics of the DVB-T receiving system is illustrated in figure 5. In contrast to the FM radio band, only channels of interest are analogically downconverted and put side by side in baseband. Then the individual DVB-T channels of interest are extracted and processed according to the proposed processing scheme. Table VI presents important parameters and numbers associated with the algorithm and the examples presented in this paper [1], and these will be referenced to in the following. Table VI shows the ambiguity distance $c/\Delta f$, combined waveform theoretical resolution $c/(N\Delta f)$, and sampling resolution c/f_s for $N = 3$ as a function of Δf.

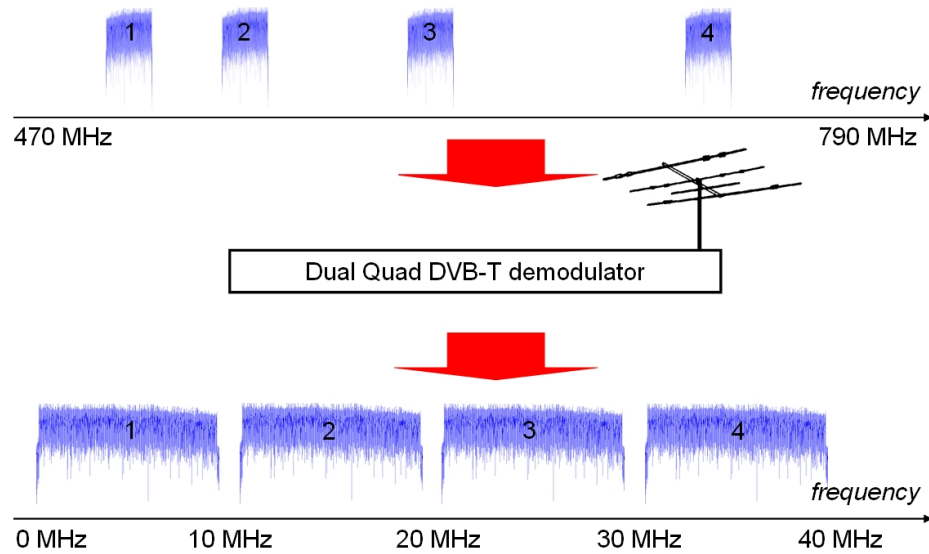Until now, the focus has been on the passive radar range cross-correlation and its properties

Fig. 5.   Schematics of the DVB-T radio case.

TABLE VI

AMBIGUITY DISTANCE $c/\Delta f$, COMBINED WAVEFORM RESOLUTION $c/(N\Delta f)$ AND SAMPLING RESOLUTION c/f_s, FOR

$N = 3$.

$[MHz]$ Δf	Ambiguity distance $c/\Delta f$	Combined distance $c/(N\Delta f)$	Sampling distance c/f_s	Ratio $f_s/\Delta f$	Ratio $\frac{f_s}{N\Delta f}$
4	75.0m	25.0m	7.5m	10.0	3.3
8	37.5m	12.5m	7.5m	5.0	1.7

in light of exploiting the available bandwidth, avoiding beamforming, signal conditioning, and adaptive cancellation. Although a simple waveform conditioning for the FM radio has been applied, it was not until the processing of the DVB-T signals started it was realized that the waveform conditioning really was necessary. The waveform conditioning is simple, the target's response across channels for the main scatterer at the same range is equalized across channels.

For real life targets, both the multipath and target RCS may be expected to be frequency dependent, and thus frequency dependent target response should be taken into account. For the FM radio PBR this is not expected to be the case to the same extent as for DVB-T, as the

frequency span is only $20MHz$, as well as the carrier frequencies are low, $88-108MHz$, for the targets of interest. However, once looking at DVB-T, the frequency span is larger, $320MHz$, as well as the frequencies higher, $470-790MHz$. From real life target analysis, it was found that the target response equalisation was necessary for the DVB-T waveform, but not for the FM radio waveform.

A. DVB-T waveform, single point target

For the FM radio case the aim of this section was to improve on the single target positioning resolution and thus indirectly also the accuracy. For the DVB-T case the resolution to begin with is so good that improving on that seems to be of less interest, [25], [26]. However, the focus will be on single target containing of multiple scatterers in order to achieve HRR capabilities, and if that is possible, the generation of ISAR images should be straightforward, once the target exhibits the necessary Doppler spreading.

The reference channels were recorded when the reference antenna was pointing at a nearby strong transmitter, and thus a strong DVB-T signal is received. Using the reference channel as signal, a synthetic target is generated in the surveillance channel at $15km$, and the bistatic range target's peak width is extracted and tabulated in table VII, i.e. the autocorrelation peak. For the single channels the $-3dB$ width is $40m$, the $-6dB$ width is $60m$, and the $-9dB$ width is $75m$, and corresponding figures are produced for the multi channel processing. It is seen that the target resolution is improved from $45m/60m/75m$ for the $-3dB/-6dB/-9dB$ peak widths respectively, to $30m/30m/45m$, for the $\Delta f = 4MHz$ case, and $15m/30m/30m$, for the $\Delta f = 8MHz$ case.

These results are directly comparable to the results from section II-A since the single scatterer in principle is the same target, only the waveform has changed. The benefits from exploiting the DVB-T waveform which offers greater bandwidths and thus resolution are clear.

However, it should be noted that the resolution is the ability to separate two echoes. In the case of a single target/scatterer, the important parameters are accuracy and lack of ambiguities. The latter is described in (2), while the former is just like for other radars, i.e. a function of the available signal-to-noise ratio as described in [21, pp. 5, accuracy].

TABLE VII

<small>AUTOCORRELATION PEAK WIDTH FOR SINGLE CHANNEL AND COMBINED CHANNELS FOR $N = 3$.</small>

		$-3dB$ peak width	$-6dB$ peak width	$-9dB$ peak width
Single	$722MHz$	45.0m	60.0m	75.0m
channel	$770MHz$	45.0m	60.0m	75.0m
	$794MHz$	45.0m	60.0m	75.0m
Multi	$\Delta f = 4MHz$	30.0m	30.0m	45.0m
channel	$\Delta f = 8MHz$	15.0m	30.0m	30.0m

B. DVB-T waveform, two point targets

Two point targets are systematically generated according to the parameters listed in table V. The surveillance channel is time-delayed N range bins, amplitude adjusted, and phase adjusted according to the delay, carrier, and target Doppler frequency. This means a second point target at another distance, but the same velocity, is mimicked. The time delay has been adjusted in accordance with the reference/surveillance channel's sampling frequency in order to avoid interpolating the delayed signal between sampling points. This was convenient in order to avoid rounding the delay to the same nearest range sample for adjacent second target delays.

The three single channel's results show that the three exploiting channels are not behaving in exactly the same way. The second scatterer is fully resolved for channels with carrier frequencies $770MHz$, and $794MHz$ at $15.060km$, while hints of the second scatterer are visible in channel corresponding to $722MHz$. Channels $722MHz$ and $794MHz$ are also fully resolving the second scatterer only at $15.038km$, and $722MHz$ also only at $15.030km$. From these results, it is hard to conclude on proper resolution capabilities, but at least $60m$ bistatic range scatterer separation should be reasonable to require. However, what is more important, is to note the difference, or gain in range resolution capabilities, which is demonstrated in figure 6, where the single channels we just described are being coherently combined.

Figure 6 is interpreted as follows: The first target is at $15km$, while the second target is stepped in range, and the actual target range is indicated in the leftmost column of the plots, numbers edgewise, i.e. the numbers $15.000, 15.008, \ldots, 15.060$. Next/below to these numbers

is the dataset duration in seconds, i.e. the numbers 0 and 0.2. The x-axis of the plots, is the processing range in kms, i.e. $14.98km$ to $15.10km$ in this example.

Figure 6a shows the case for the combination of three, $N = 3$, channels with $\Delta f = 4MHz$. The target second scatterer is stepped in range from $15km$ (single target) to $15.060km$. The second scatterer is clearly resolved already for $15.030km$, although at a slightly wrong range, but this is probably due to the fact that the second scatterer is interacting with the main scatterer at $15.000km$, as well as the effective rounding to the closest range sampling. It is noted that due to the overlapping frequency spectra, little range sidelobes and ambiguities are experienced.

For the $N = 3$, and $\Delta f = 8MHz$ case, it is seen that the second scatterer have impact at the plot already at $15.008km$, strongly at $15.015km$, but the second scatterer is not fully resolved before $15.023km$, although the ambiguity situation is slightly worse than for the $\Delta f = 4MHz$ case. The ambiguity distance, table VI, is $37.5m$, and thus folding of the second target around this distance should be present. There are some signs of this effect, however less pronounced than expected.

By using overlapping/adjacent bands $\Delta f < B/2$, some of the ambiguities in the range correlation is avoided, while by allowing frequency gaps, $\Delta f > B/2$, ambiguities which may complicate the picture are introduced. How to properly tune this will be the radar designer's choice to make once the application has been decided.

The combination of multiple DVB-T channels in the range correlation improves on the PBR system's capabilities to resolve nearby scatterers. With respect to the single channels resolution performances, being around $60m$ in bistatic range, the combined channels resolution performance from figure 6 is seen be be $30m/23m$ for the $\Delta f = 4MHz/\Delta f = 8MHz$ by using three non-adjacent DVB-T channels in the range correlation with varying frequency spacing.

C. DVB-T waveform, summary

Simulation results from using real life DVB-T recorded signals have been presented. The focus has been on mapping the DVB-T waveform's behavior and performance in the proposed algorithm by using real life strong recorded broadcast signals from nearby broadcasters.

By exploiting multiple broadcast channels the simulations show that the single point scatterer resolution is improved from $45m/60m/75m$ for the $-3dB/-6dB/-9dB-$ single channels
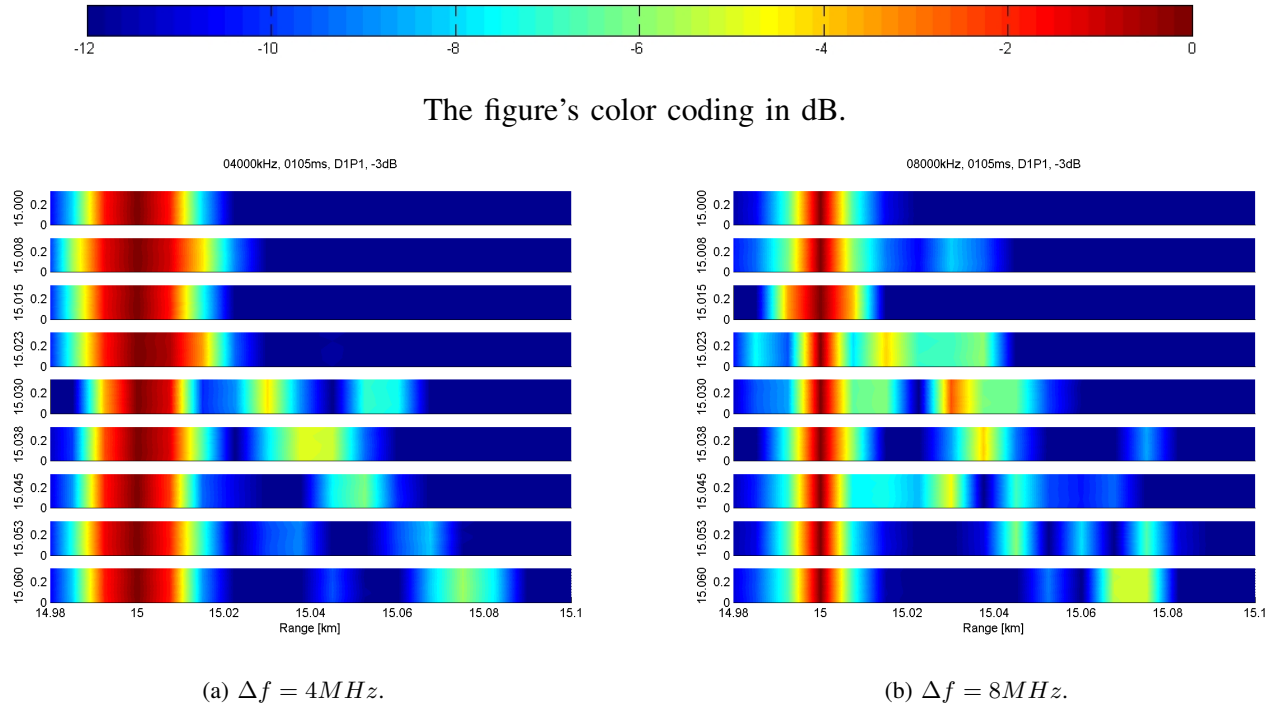
Fig. 6. Systematic testing of the algorithm's resolution capabilities for two scatterers with varying range, and one $3dB$ below the first, parameters varying according to table V. CPI$= 105ms$, $N = 3$.

target peak widths to $30m/30m/45m$, for the $\Delta f = 4MHz$ case, and $15m/30m/30m$, for the $\Delta f = 8MHz$ case. All results are tabulated in table VII.

It is also shown that the combination of multiple DVB-T channels in the range correlation improves on the PBR system's capabilities to resolve nearby scatterers. The resolution capabilities was improved from around $60m$ to $30m/23m$ for the $\Delta f = 4MHz/\Delta f = 8MHz$ by using three DVB-T channels in the range correlation with varying spacing. The theoretical range performance of the algorithm is summarized in table VI. By using overlapping/adjacent bands $\Delta f < B/2$, some of the ambiguities in the range correlation is avoided, while by allowing frequency gaps, $\Delta f > B/2$, ambiguities which may complicate the picture are introduced. How to properly tune this will be the radar designer's choice to make once the application has been decided.

IV. CONCLUSION

Simulations based on real life FM radio waveforms showed that the algorithm is capable of improving range resolution, and thus the accuracy, according to theory for single scatterers as is summarized in table IV. The performance of the algorithm was impacted by the fluctuating

behavior of the FM radio signal, although less than expected. The simulations also showed that two targets not resolved in the individual channels, are resolved by using the proposed algorithm properly. Single scatterer targets may be significantly better positioned by the improved resolution (and in consequence also the accuracy) capabilities, i.e. ten times of the best performing individual channel.

The algorithm's performance with the DVB-T waveform was more predictable due to the noise like modulation offered by the coded orthogonal frequency-division multiplexing in contrast to the content dependent FM. All simulation results are tabulated in table VII, where it is shown that for the DVB-T waveform, single scatterer targets will be up to three times more accurately positioned by the increased range resolution algorithm, $-3dB$ target peak width down to $15m$ ($7.5m$ equivalent monostatic range resolution) compared to single channel range processing, target $-3dB$ peak width of $45m$ ($22.5m$ equivalent monostatic range resolution), for the three DVB-T channels in this example. It is expected that similar accuracy improvements can be achieved, as for traditional systems, [21, pp. 5, accuracy].

Considering multiple targets and/or multiple scatterer targets, the simulations showed that the DVB-T waveform and current processing algorithms offers target separation, i.e. bistatic target peak widths of around $60m$. The two examples provided in this work showed target resolution capabilities of $30m$ and $23m$. By using the monostatic equivalent range resolution the numbers corresponds to $30m$ improved down to $15m$ and $11.5m$, meaning targets separated by around $10m$ distance will be resolved in *range*, before Doppler separation is considered.

REFERENCES

[1] K. E. Olsen and K. Woodbridge, "Performance of a Multiband Passive Bistatic Radar Processing Scheme - Part I," *IEEE AESS Systems Magazine Special Issue on PCL*, August 2011.

[2] K. E. Olsen and C. J. Baker, "FM-based passive bistatic radar as a function of available bandwidth," in *Proc. of IEEE Radar Conference*, May 2008, invited paper.

[3] K. E. Olsen and K. Woodbridge, "FM based passive bistatic radar target range improvement," in *Proc. International Radar Symposium*, September 2009.

[4] K. E. Olsen, K. Woodbridge, and I. A. Andersen, "FM Based Passive Bistatic Radar Target Range Improvement - Part II," in *Proc. International Radar Symposium*, June 2010.

[5] K. E. Olsen and K. Woodbridge, "FM Based Passive Bistatic Radar Target Range Resolution Improvement - Part III," in *Proc. International Radar Symposium*, September 2011.

[6] M. Cherniakov, Ed., *Bistatic Radar: Emerging Technology*. John Wiley & Sons Ltd, 2008.

[7] K. E. Olsen and K. Woodbridge, "Analysis of the Performance of a Multiband Passive Bistatic Radar Processing Scheme," in *IEEE Waveform Diversity & Design Conference*, August 2010.

[8] *Transmission standards for FM sound broadcasting at VHF - Recommendation ITU-R BS.450-3*, International Telecommunication Union (ITU) Std., 2001. [Online]. Available: http://www.itu.int

[9] (2008, March) FM broadcasting. Wikipedia. [Online]. Available: http://en.wikipedia.org/wiki/FM_broadcasting

[10] H. Stark, F. B. Tuteur, and J. B. Anderson, Eds., *Modern Electrical Communications - Analog, Digital and Optical Systems, Second Edition*. Englewood Cliffs, New Jersey 07632: Prentice Hall, 1998.

[11] E. Blossom. (2004, September) Listening to FM Radio in Software, Step by Step. Linux Journal. [Online]. Available: http://www.linuxjournal.com/article/7505

[12] H. D. Griffiths, "From a different perspective: Principles, practice and potential of bistatic radar," in *Proc. International Radar Conference*, September 2003.

[13] C. J. Baker and H. D. Griffiths, "Bistatic and Multistatic Radar Sensors for Homeland Security," in *NATO Advanced Study Institute, Advances in Sensing with Security Applications*, July 2005.

[14] H. D. Griffiths and C. J. Baker, "Passive coherent location radar systems. Part 1: Performance prediction," *IEE Proc.-Radar Sonar Navig.*, vol. 152, no. 3, pp. 153–159, June 2005.

[15] C. J. Baker, H. D. Griffiths, and I. Papoutsis, "Passive coherent location radar systems. Part 2: Waveform properties," *IEE Proc.-Radar Sonar Navig.*, vol. 152, no. 3, pp. 160–168, June 2005.

[16] H. D. Griffiths and C. J. Baker, "The Signal and Interference Environment in Passive Bistatic Radar," in *Information, Decision and Control, IDC'07*, February 2007.

[17] R. Saini and M. Cherniakov, "DTV signal ambiguity function analysis for radar application," *IEE Proc.-Radar Sonar Navig.*, vol. 152, no. 3, pp. 133–142, June 2005.

[18] A. Lauri, F. Colone, R. Cardinali, C. Bongioanni, and P. Lombardo, "Analysis and Emulation of FM Radio Signals for Passive Radar," in *Aerospace Conference, 2007 IEEE*, March 2007.

[19] T. Tsao, M. Slamani, P. Varshney, D. Weiner, H. Schwarzlander, and S. Borek, "Ambiguity function for a bistatic radar," *IEE Trans. Aerospace and Electronic Systems*, vol. 22, no. 3, pp. 1041–1051, July 1997.

[20] D. R. Wehner, *High-Resolution Radar*, 2nd ed. Norwood, MA, USA: Artech House, 1995.

[21] D. K. Barton and S. A. Leonov, Ed., *Radar Technology Encyclopedia*, 1st ed. Artech House, Inc, 1997.

[22] *Digital Video Broadcasting (DVB); Framing structure, channel coding and modulation for digital terrestrial television. ETSI EN 300 744 V1.5.1 (2004-11)*, The European Telecommunications Standards Institute (ETSI) Std., 2004. [Online]. Available: http://www.etsi.org

[23] J. M. Christiansen and K. E. Olsen, "Range and Doppler walk in DVB-T based Passive Bistatic Radar," in *Radar Conference, 2010. RADAR '10. IEEE*, May 2010.

[24] J. M. Christiansen, "DVB-T based Passive Bistatic Radar. Simulated and experimental data analysis of range and Doppler walk," Master's thesis, NTNU, Norwegian University of Science and Technology, 2009.

[25] J. Ferrier, M. Klein, and S. Allam, "Frequency and Waveform Complementarities for Passive Radar Applications," in *International Radar Symposium 2009*, September 2009.

[26] H. Kuschel, J. Heckenbach, D. O'Hagan, and M. Ummenhofer, "A Hybrid Multi-Frequency Passive Radar Concept for Medium Range Air Surveillance," in *PCL Focus Day*. Franhofer FHR, May 2011.